ORIGINAL PAPER

Characterization and physiochemical studies of crosslinked thiolated polyvinyl alcohol hydrogels

Bhuvanesh Gupta · Sadiya Anjum · Saiqa Ikram

Abstract Modification and crosslinking of polyvinyl alcohol (PVA) by thiolation using thioglycolic acid (TGlA) and various crosslinkers were carried out. The crosslinked thiolated PVA (TPVA) hydrogels were characterized by thermogravimetric analysis (TGA), differential scanning calorimetry (DSC), X-ray diffraction (XRD) and Fourier transform infra red spectroscopy coupled with thermal analysis (TG-FTIR) techniques. The crosslinking of the resultant material was carried out using three crosslinker sodium trimetaphosphate (STMP), glyoxal and boric acid. The influence of esterification and crosslinking on the physical and chemical properties of the material was studied. XRD showed that after crosslinking the crystallinity of TPVA hydrogels decreased. These results were further substantiated by DSC observations. The thermal stability of the TPVA hydrogels is enhanced. A significant variation in the initial decomposition temperature was observed with respect to different STMP crosslinked samples having varying TGlA concentration and different crosslinkers. The coupled TG-FTIR studies of crosslinked samples at different temperatures show that the evolution of sulfur-containing gases (carbon disulfide and carbon monosulfide) is being prominent for this material.

Keywords Polyvinyl alcohol · Thioglycolic acid · Esterification · Crosslinking · Thiol content · Swelling

B. Gupta (✉)
Bioengineering Laboratory, Department of Textile Technology, Indian Institute of Technology, New Delhi 110016, India
e-mail: bgupta@textile.iitd.ernet.in

S. Anjum · S. Ikram
Department of Chemistry, Jamia Millia Islamia (Central University), New Delhi 110025, India

🖄 Springer

Introduction

In recent years, interest in developing new polymeric materials in water treatment applications has increased considerably. Polyvinyl alcohol (PVA) has found significant applications in different areas such as textile sizing and finishing agents, emulsifier, photosensitive coating, and adhesives for paper, wood, textiles, and leather [1, 2]. Moreover, it is a biologically favorable polymer due to its full biodegradability and biocompatibility [3]. These properties are, however, counter balanced by the poor stability of PVA in wet stage, which renders the application of PVA in water treatment.

Several efforts using processes like blending and chemical modification were employed to make PVA insoluble [4–6]. The most common modification reactions for PVA are esterification, etherification or acetalization of the hydroxyl groups. Esterification of PVA with acid chloride, anhydride and carboxylic acid has been widely studied [7–10]. The extent of modification of the surface as well as bulk can be controlled by proper selection of reaction conditions. In addition to esterification of PVA, crosslinking is another key to improve the structural integrity of the modified PVA in aqueous medium. Several crosslinkers that are well known for the crosslinking of PVA include phosphoryl chloride, epichlorohydrin, sodium trimetaphosphate (STMP) and aldehydes [11–16]. However, it is important to study the structural changes occurring in the polymer matrix due to the modification process.

Shengju et al. investigated the preparation and characterization of novel mesoporous PVA/SiO$_2$ composite nanofiber membranes via sol–gel electrospinning method, intended to increase the adsorption of heavy metal ions from waste water [17]. Yoon et al. investigated the preparation of starch/PVA blend films plasticized by glycerol and crosslinked by glutaraldehyde and STMP. The crosslinking evidence of STMP with PVA/PVP was confirmed by FTIR and mechanical studies [18]. Uslu et al. [19] carried out the characterization of PVA/boron fiber produced by the electrospinning method by SEM, differential scanning calorimetry (DSC) and FTIR studies. Quantitative analysis of glyoxal crosslinked PVA was described in this report. A convenient FTIR method has been established to analyze the degree of crosslinking in PVA [20]. Miyazaki et al. [21] stated the role of boric acid on the melting behavior of PVA film by the comparative studies of X-ray diffraction (XRD) and DSC. Zhang et al. [22] reported the negative biodegradation of PVA modified by various aldehydes. The modification was observed by FTIR due to the formation of covalent acetals. Thermal degradation mechanism of PVA/silica nanocomposite has been studied by coupled FTIR/TG analysis. Evaluation of gases at different degradation steps has been successfully reported by this coupled technique [23].

The introduction of thiol groups into the PVA matrix may produce considerable changes in the inherent properties of the base material. In our previous work, we have carried out the esterification and subsequent crosslinking of the matrix by different crosslinkers [24, 25]. Various conditions, like reaction time, reaction temperature, reactants concentration and nature of crosslinkers were optimized. In this study, we have attempted to observe structural changes obtained by two-step

modification of PVA. The crosslinked thiolated PVA (TPVA) films were characterized by TGA, DSC, XRD and coupled thermogravimetric-Fourier transform infrared (TG-FTIR) techniques.

Experimental

Chemicals

PVA (Mw 150,000 and degree of hydrolysis 85 %) and sodium trimetaphosphate were purchased from Sigma Aldrich. Thioglycolic acid (TGlA), sodium hydroxide, sulfuric acid (H_2SO_4), glyoxal (GLY), potassium thiocyanate, silver nitrate, iron ammonium sulfate hexahydrate and methanol (HPLC grade) were purchased from Merck, India. Boric acid (BA) was purchased from S.D Fine Chemicals, India. All the chemicals were used without further purification. Ultra-pure water, resistivity less than 18 MΩ cm, produced by a Millipore Milli-Q system was used throughout the experimental work.

Preparation of crosslinked thiolated PVA

Thiolated PVA was prepared by the reaction of PVA with TGlA and subsequent crosslinked with different crosslinkers. Homogenous solution of PVA was prepared in water under vigorous stirring at room temperature. Esterification reaction was carried out with PVA concentration 2 % (w/v), TGlA 25 % (v/v) at a temperature of 60 °C 24 h in the presence of (H_2SO_4) catalyst 1 % (v/v). The esterified PVA solution was used later on for crosslinking with different crosslinker at 0.1 % (w/v) under constant stirring for 30 min. After completion of the reaction, the mixture was slowly poured into 12 M sodium hydroxide solution at pH 12. A white precipitate was collected, washed repeatedly with water, methanol and dried in a vacuum oven at room temperature [24, 25].

In the present investigation, the thiol content was determined according to a protocol based on the Volhard's silver nitrate method [26]. The determination is based on the chemical affinity of silver towards thiol groups. The swelling studies of crosslinked TPVA were assessed by the gravimetric method. The swelling study of the sample was mentioned as a function of time. The swelling percent of the sample was calculated using the following equation [27]:

$$\text{Swelling } (\%) = \frac{W_s - W_d}{W_d} \times 100, \tag{1}$$

where W_s and W_d are the weight of the samples in the swollen and dry states, respectively.

Differential scanning calorimetry

Differential scanning calorimetry studies of the samples were carried out on DSC-204 F1 Phoenix, Netzch, Germany system. About 5–10 mg samples were loaded in

the aluminum pan and the thermograms were run in the temperature range 30–300 °C at a heating rate of 10 °C/min. The heat of fusion (ΔH_f) was obtained from the area under the melting thermogram. The crystallinity of the samples was obtained by the following expression:

$$\% \text{ Crystallinity } = \frac{\Delta H_f}{\Delta H_{f(\text{crys})}} \times 100, \tag{2}$$

where ΔH_f is the heat of fusion of the sample and ΔH_f (crys) is the heat of fusion of 100 % crystalline PVA and was taken as 138 cal/g [28].

X-ray diffraction studies

X-ray diffractograms of the samples were recorded on a PHILIPS, Holland, CuKα X-ray generator to study morphological changes in the material. Scanning was carried out in 2θ range of 5°–35° at a wavelength of 1.54 Å, filament current of 30 mA and voltage of 40 kV. The crystallinity of the samples was obtained by the following expression [27]:

$$\% \text{ Crystallinity} = \frac{\text{Crystalline area}}{\text{Total area}} \times 100. \tag{3}$$

Thermogravimetric analysis (TGA)

Thermogravimetric analysis studies were carried out using a Perkin–Elmer TGA-7 system in the range of 50–600 °C. The heating rate was 10 °C/min. The measurements were made under a constant flow rate (20 ml/min) of nitrogen. The initial decomposition temperature (IDT) was obtained as the tangent at a point where the weight loss starts.

Thermogravimetric-Fourier transform infrared studies

Thermogravimetric-Fourier transform infrared measurements of the crosslinked TPVA samples were performed on a NETZSCH TG 209 *F1Iris*® simultaneously coupled to the BRUKER Optics FTIR *TENSOR*™. The decomposition gases from each degradation step were transferred from TGA analyzer at temperature range 30–600 °C (20 K/min), and measured by FTIR spectrometer in the scanning wave number range of 4,000–600 cm^{-1}.

Results and discussion

The characterization of the uncrosslinked and crosslinked TPVA samples was carried out to investigate the physical and chemical changes that are incorporated in the material after esterification and simultaneous croslinking. Distinct changes in the physical structure of PVA have been observed by different studies. The other factor guiding the investigation has been the variation of thiol content with different

crosslinkers under identical conditions. The effect of different crosslinkers on various physical and chemical properties of crosslinked TPVA has also been discussed.

Influence of acid concentration

XRD studies

X-ray diffractograms of pure PVA, TPVA and STMP crosslinked TPVA hydrogels (STMP-TPVA) are shown in Fig. 1. The thiol content of TPVA and STMP-TPVA samples was calculated to be 3.9 and 3.5 mmol/g, respectively. The lower amount of thiol in STMP crosslinked samples is due to the diminishing accessibility of thiol groups within the crosslinked matrix [25]. The appearance of sharp reflections, evident from the XRD of pure PVA, is characteristic of crystalline and amorphous phases of conventional semi-crystalline polymers. Moreover, the pattern observed for pure PVA shows several distinct crystalline peaks at $2\theta = 14°$, $16°$, $25°$ and $28°$. The XRD scan of pure PVA clearly shows the semicrystalline nature of PVA.

The XRD scans for the thiolated samples showed two peaks at $14°$ and $16°$ which revealed the crystal structure of PVA. The first peak in PVA structure at $14°$ disappears and second is gradually shifted toward $19°$, indicating the distortion of crystalline structure after simultaneous modification. The crystalline reflections for STMP crosslinked TPVA were found to occur at distinct angles identical to TPVA. However, the crystallinity could be visualized to diminish as a result of crosslinking process. Other authors have also observed the amorphous nature of STMP-induced crosslinking process [29].
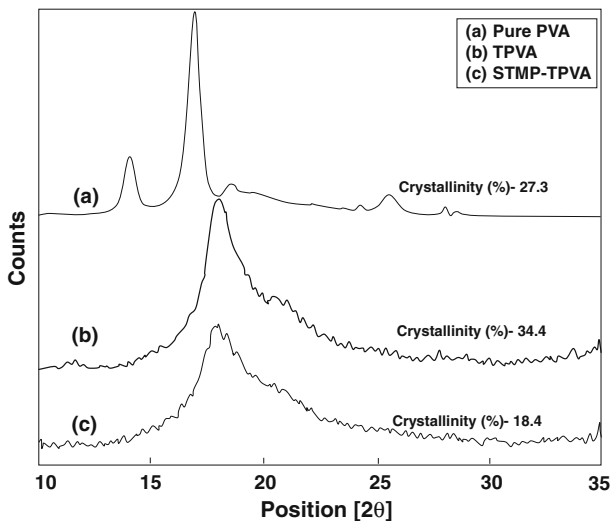

Fig. 1 X-ray diffractogram of **a** pure PVA, **b** uncrosslinked TPVA and **c** STMP-TPVA. Reaction conditions: PVA 2 % (w/v), TGlA 25 % (v/v), crosslinker content 0.1 % (w/v), crosslinking time 30 min

TGA studies

The TGA results for pure PVA, TPVA and STMP-TPVA hydrogels are shown in the Fig. 2. Pure PVA showed a two-step decomposition pattern. The first step started at the beginning of the thermogram and continued up to 200 °C and the second step began around 240 °C. The first step of weight loss could be attributed to the loss of water, which may involve the moisture and the dehydration involving two hydroxyl groups leading to the intramolecular as well as intermolecular cyclization. The cyclization has already been observed by other groups and hence supports our investigation [23]. The second step was mainly caused by the decomposition of the molecular chains. TGA thermogram shows that the thermal stability of pure PVA is increased after esterification and crosslinking reaction. Initial weight loss in the samples (50–200 °C range) is lower than pure PVA and could be explained by lower moisture content due to the crosssinking reaction.

DSC studies

DSC thermograms of the pure PVA, crosslinked and uncrosslinked TPVA samples with varying thiol content are presented in Fig. 3. The glass transition temperature T_g of pure PVA has been observed at 70 °C, which is similar to the one reported by other workers [30, 31]. After thiolation of PVA, T_g decreased due to the formation of strong covalent bond while after crosslinking the T_g value continuously decreases due to the diminishing degree of crystallinity.

Pure PVA shows a sharp endothermic peak at 190 °C. However, after esterification, TPVA films indicated a new broad peak at the lower temperature zone (150–180 °C), which can probably be assigned to melting of the quasi-crystalline phase. The quasi-crystalline phase can be regarded as defects in the pure PVA crystalline phase. Uncrosslinked TPVA shows melting at 205 °C. Further DSC studies of STMP crosslinked samples show a rapid decrease in the glass transition
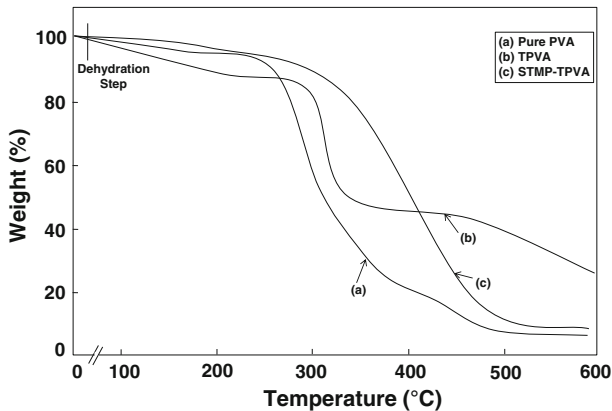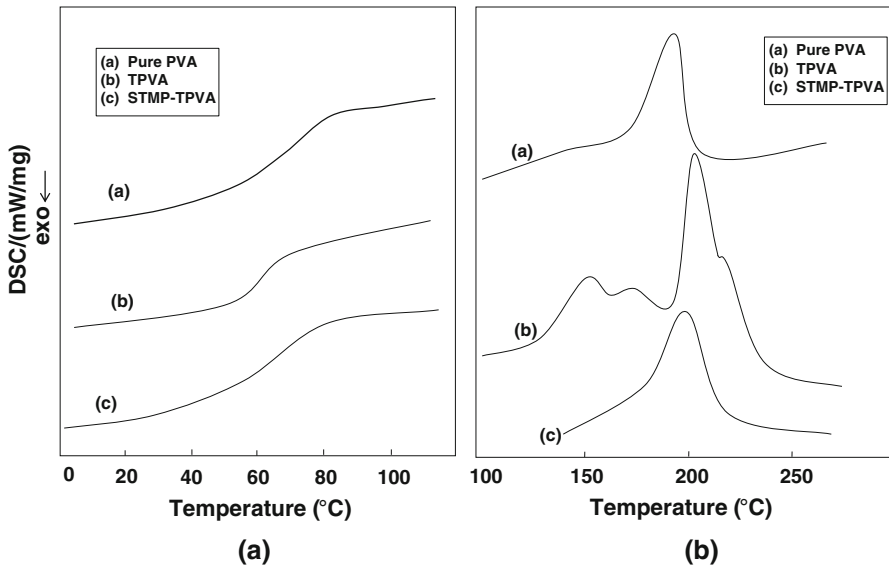

Fig. 2 TGA thermogram of **a** pure PVA, **b** uncrosslinked TPVA and **c** STMP-TPVA. Reaction conditions: PVA 2 % (w/v), TGlA 25 % (v/v), crosslinker content 0.1 % (w/v), crosslinking time 30 min

Fig. 3 DSC thermogram on glass transition and melting temperature region of **a** pure PVA, **b** uncrosslinked TPVA and **c** STMP-TPVA. Reaction conditions: PVA 2 % (w/v), TGlA 25 % (v/v), crosslinker content 0.1 % (w/v), crosslinking time 30 min

Table 1 Description of DSC thermograms of (a) pure PVA, (b) uncrosslinked TPVA and crosslinked TPVA (c) STMP-TPVA, (d) BA-TPVA, (e) GLY-TPVA

Sample	Thiol content (mmol/g)	T_g (°C)	T_m (°C)	ΔH (J/g)	Crystallinity (%)
Pure PVA	–	83	191	39.7	29.2
TPVA	3.9	70	205	45.7	31.2
STMP-TPVA	3.5	65	175	22.8	16.6
BA-TPVA	3.1	61	177	24.8	17.8
GLY-TPVA	2.9	45	165	37.2	26.9

Reaction conditions: PVA 2 % (w/v), TGlA 25 % (v/v), crosslinker content 0.1 % (w/v), crosslinking time 30 min

temperature (T_g), enthalpy of fusion (ΔH_f) and melting temperature (T_m) due to the absence of this quasi-crystalline phase and structure deformation. Details of the above-stated DSC studies are tabulated in Table 1.

Influence of the nature of the crosslinker

XRD studies

The XRD patterns of crosslinked TPVA samples with different crosslinker are presented in Fig. 4. The thiol content of these samples is in the range of
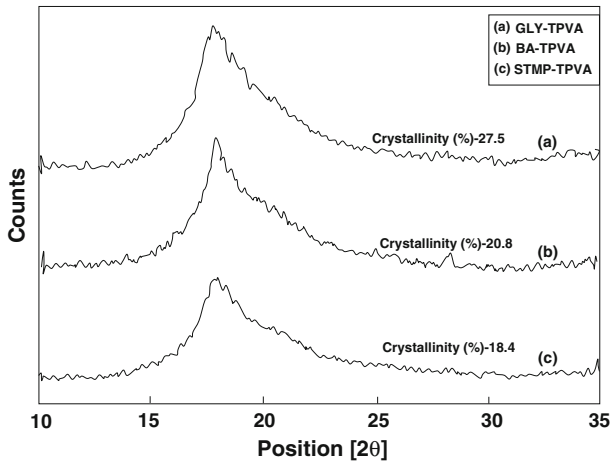
Fig. 4 X-ray diffractograms of crosslinked TPVA samples **a** GLY-TPVA, **b**, BA-TPVA, **c** STMP-TPVA. Reaction conditions: PVA 2 % (w/v), TGlA 25 % (v/v), crosslinker content 0.1 % (w/v), crosslinking time 30 min

2.5–3.5 mmol/g. The action of three crosslinkers is similar but the magnitude of their impact is different. The crystallinity of both the GLY and BA crosslinked samples was lower than the crystallinity of STMP crosslinked samples. It seems that GLY leads to more efficient interlinking of chains due to the covalent crosslinking of groups. The aldehyde groups of glyoxal form covalent acetal bonds with the hydroxyl groups of PVA and the resonance established with adjacent double ethylenic bonds via a Schiff reaction [20]. While BA and STMP both form ionic bonds like borate and phosphate linkages, respectively, with the hydroxyl groups of PVA. Ionic crosslinking is a simple and mild procedure in contrast to covalent crosslinking; therefore, the crystallization process is hindered to some extent [32].

DSC studies

DSC thermograms showing T_g and T_m separately for the crosslinked TPVA samples with different crosslinkers are presented in Fig. 5 and also tabulated in Table 1. In order to explain these results, one has to take into account that the studied system is a very complex one. It is known that PVA is a semicrystalline polymer in which high physical interactions between the polymer chains are present due to hydrogen bonding between the hydroxyl groups [33].

The introduction of a different crosslinking agent affects both the crystallinity and physical networking of the system. The crosslinking increases the rigidity and the new moieties introduced can affect T_g in a different way, depending on their bonding strategies. In our case, all three crosslinkers, STMP, BA and GLY, created the bridges between the polymer chains which are not rigid ones, but flexible sequences of phosphate, borate and acetal formation, respectively.

Parallel DSC studies show a rapid decrease in the enthalpy of fusion ΔH_f and melting temperature T_m which testify to the loss of crystallinity with crosslinking
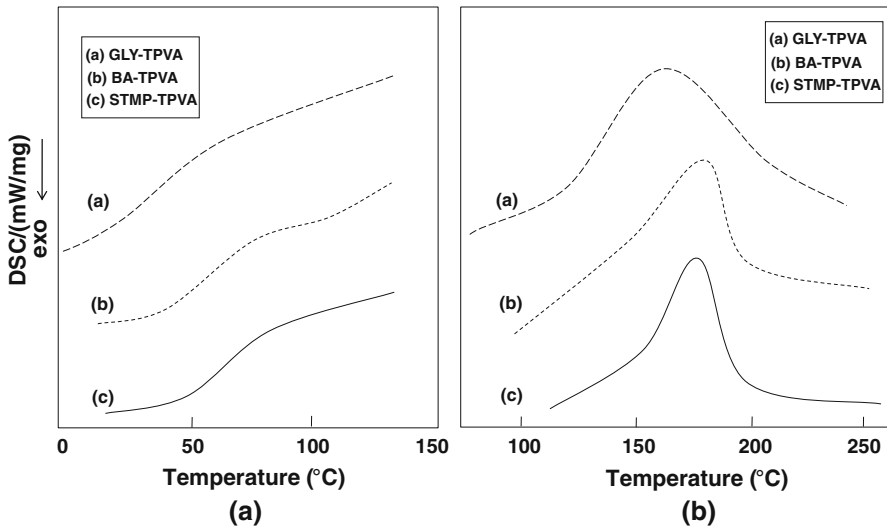
Fig. 5 DSC thermogram in glass transition region and melting region of TPVA crosslinked samples **a** GLY-TPVA, **b** BA-TPVA, **c** STMP-TPVA. Reaction conditions: PVA 2 % (w/v), TGlA 25 % (v/v), crosslinker content 0.1 % (w/v), crosslinking time 30 min

[32]. This may be due to that the crosslinker must hinder the crystallite growth in the molecular chain because crosslinking points cannot be included in crystalline domains. It has been reported by several authors that the crystallinity of crosslinked samples decreases with crosslinking [21, 34]. In crosslinking with GLY, the endothermic peak of TPVA decreased along with the depression of the melting temperature. However, the total crystallinity region is higher than the other two crosslinkers.

TG-FTIR studies

The coupled TG-FTIR study was used and the on-line analysis of the evolved gases from material was performed. Figure 6 depicts the relative mass change of the pure PVA sample and the Gram–Schmidt trace as a function of the overall IR intensities. Gram–Schmidt plots are useful as they provide information related to the total IR absorbance of the evolved components over the entire spectral range [35].

There are three distinct and well-separated regions (80–140 °C, 300–450 °C and 450–550 °C) in the thermogravimetry. These may be correlated with the three-step-degradation. To avoid the overlap of evolved gases from different degradation steps, the samples were heated at three temperature points, 145, 345 and 476 °C, with reference spectra from the NIST database. The spectra are shifted in the absorbance axis. Figure 7 shows the comparative spectra of the evolved gases during PVA heating with reference water at temperature 145 °C. This indicates the elimination of residual water from the matrix indicating the dehydration process take place.

FTIR spectra of pure PVA at 345 °C are shown in Fig. 8. However, as the present study employs (85–88 %) hydrolyzed PVA, a large amount of acetate groups
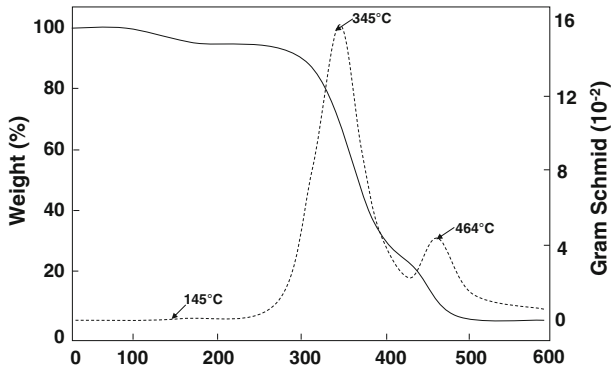
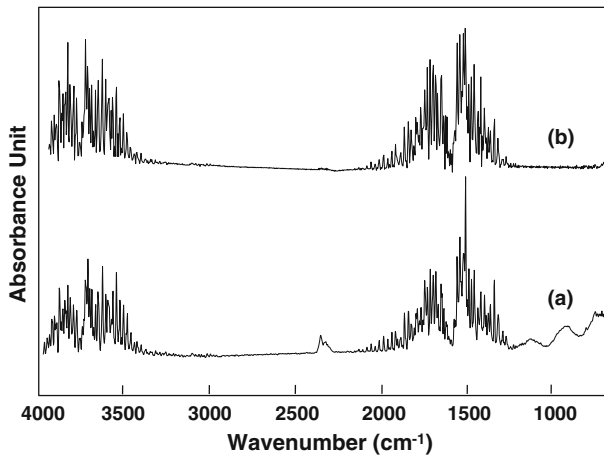**Fig. 6** TG thermogram of pure PVA (*continuous line*) and Gram–Schmidt trace (*dotted line*)

Fig. 7 FTIR spectrum at 145 °C pure PVA (**a**) with the reference spectrum of water (**b**)

remain in PVA chains. As the acetate groups are randomly inserted between hydroxyl groups, the elimination of H_2O and residual acetate groups occurs simultaneously. In addition to water, a large amount of acetic acid is also observed during the first degradation step. The narrow and intense peaks at 3,550 and 1,760 cm^{-1} correspond to the stretching vibration peaks of OH and COO^- of gaseous acetic acids, respectively [36].

The comparative FTIR spectra of pure PVA at 464 °C are shown in Fig. 9. The pure PVA displays absorbance peaks in the region of 2,395–2,268 cm^{-1}. This is representative of CO_2 due to the asymmetric stretching of the carbonyl group [37]. Carbon monoxide which is represented by the functional group CO at the absorption band between 2,240 and 2,060 cm^{-1} was present. The CO functional group is representative of carbon monoxide as detailed by several authors [38–40]. As anticipated, the FTIR spectra exhibit increased levels of CO with the high temperature pyrolysis of PVA.
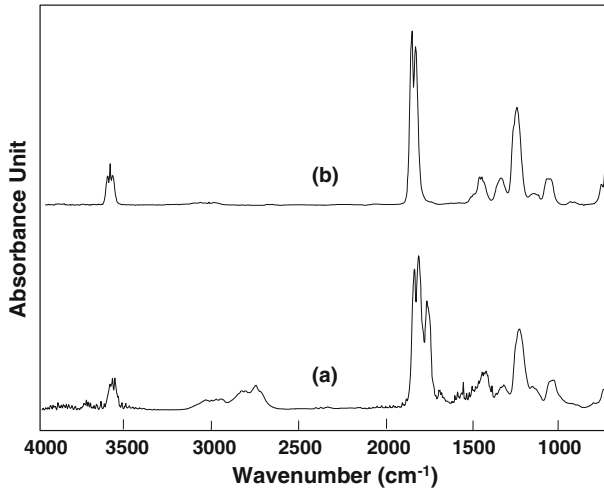
Fig. 8 FTIR spectrum at 345 °C of pure PVA (**a**) with reference spectra of acetic acid (**b**)
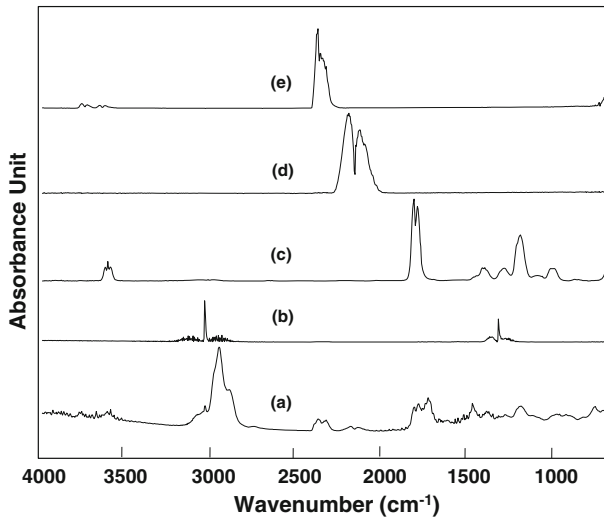

Fig. 9 FTIR spectrum at 464 °C pure PVA (**a**) and reference spectra of methane (**b**), acetic acid (**c**), carbon monoxide (**d**) and carbon dioxide (**e**)

TG and Gram–Schmidt curve of crosslinked TPVA sample with different crosslinkers having varying thiol content are presented in Fig. 10. The thermograms of three samples STMP-TPVA, BA-TPVA and GLY-TPVA have nearly the same decomposition behavior. To compare the evolved gases of the above three samples, the FTIR spectra in the region below 200 °C, about 275, 385 and 470 °C are shown separately in the next four figures with the most relevant reference substances from the NIST database (Figs. 11, 12, 13, 14). Figure 11 shows the FTIR spectra of crosslinked TPVA samples below 200 °C where all samples evolved water. The
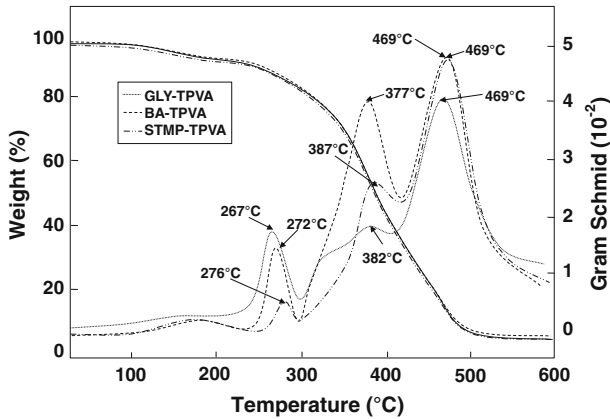
Fig. 10 TG thermograms and Gram–Schmidt traces of crosslinked TPVA samples
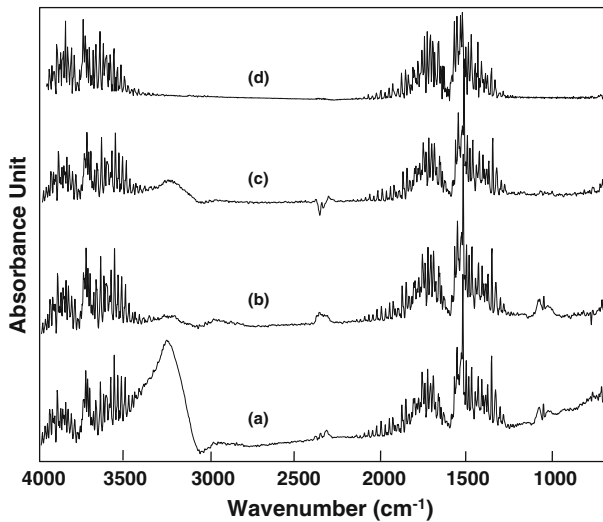
Fig. 11 FTIR spectra below 200 °C of GLY-TPVA (**a**), STMP-TPVA (**b**), BA-TPVA (**c**) and water (**d**)

intense peak appearing at a wavenumber of 3,300 cm^{-1} is due to ice on the MCT detector.

The FTIR spectra of crosslinked TPVA samples at 275 °C are shown in Fig. 12. This spectrogram is highly relevant to exhibit the evolution of sulfur-containing gases from this material. The CS_2 evolution is investigated at 1,575–1,500 cm^{-1} and the liberation of C–O–S is observed at 2,150–2,050 cm^{-1} [41, 42]. With respect to the TGA-FTIR spectra, the present study was not able to detect H_2S, SO_2 and any other relevant sulfur-containing gas.

The FTIR spectra of different crosslinked samples at 385 °C are shown in Fig. 13. The spectra show the increased intensity of acetic acid, CO_2 and CO as compared with pure PVA due to the greater involvement of the respective
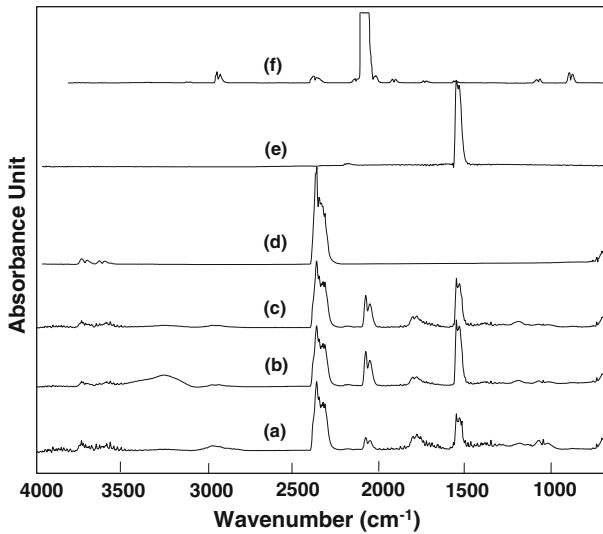
Fig. 12 FTIR spectra at about 275 °C of GLY-TPVA (**a**), STMP-TPVA (**b**), BA-TPVA (**c**), carbon dioxide (**d**) carbon disulfide (**e**) and COS (**f**)
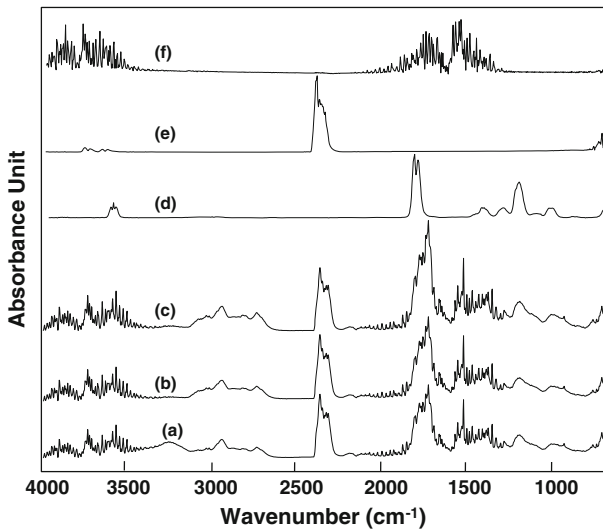

Fig. 13 FTIR spectra at about 385 °C of GLY-TPVA (**a**), STMP-TPVA (**b**), BA-TPVA (**c**), acetic acid (**d**), carbon dioxide (**e**) and water (**f**)

components in the system. The band appearing in the range of 2,240–2,060 cm^{-1} is due to the liberation of CO_2 gas when the material decomposes at this temperature. Figure 14 represents the FTIR spectra of the above-mentioned samples at a very high temperature of 470 °C. At this temperature, all the materials are completely
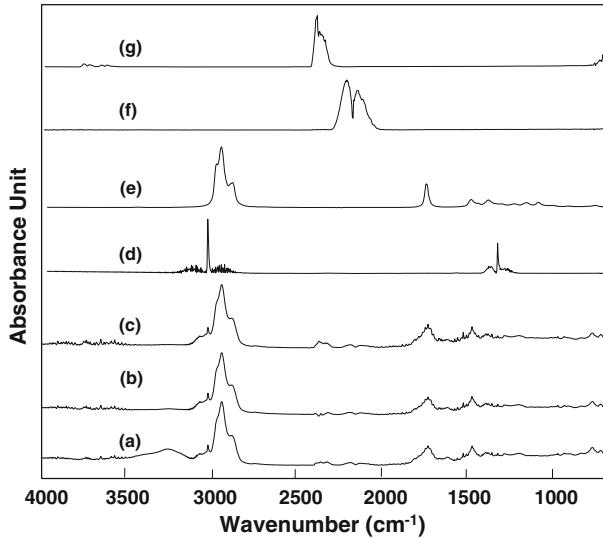
Fig. 14 FTIR spectra at about 470 °C of GLY-TPVA (**a**), STMP-TPVA (**b**), BA-TPVA (**c**), methane (**d**), 7-Tridecanone (**e**), carbon monoxide (**f**) and carbon dioxide (**g**)

decomposed. In the spectral range of $3,100–2,900\ \text{cm}^{-1}$, this can be seen by the evaluation of methane.

Conclusion

In summary, we demonstrated a novel approach for the preparation of crosslinked TPVA hydrogels, functionalized with thiol groups. The thermal stability of the unmodified PVA was increased after simultaneous modification. At the same time, rapid decrease in the ΔH_f, T_g and T_m was observed indicating the diminution of crystallinity with crosslinking. This may be due to the binding of PVA chains which restricts the arrangement of chains due to the crystal structure. The XRD and DSC studies reveal that different crosslinkers show distinct nature of bonding like ionic and covalent; therefore, BA and GLY show more crystalline nature as compared with the STMP. The coupled TG-FTIR studies of crosslinked samples were used for the analysis of the evolved gases from the material in different temperature ranges with the most relevant reference substances from the NIST database. The most important representation of this spectrogram is to show the evolution of sulfur-containing gases being prominent for this material. The evolution of CS_2 and COS was investigated at their respective range. With respect to the TG-FTIR spectra, the present study was not able to detect H_2S, SO_2 and any other relevant sulfur-containing gas. It is seen that the simultaneous modification process is a useful tool for improving the performance of hydrogel. Consequently, this hydrogel can be a promising material for removing and recovering arsenic ions from water [43].

References

1. Katia CS, Figueiredo LM, Alves C, Borges P (2009) Poly(vinyl alcohol) films crosslinked by glutaraldehyde under mild conditions. J Appl Polym Sci 111:3074–3080. doi:10.1002/app.29263
2. Xiao S, Huang RYM, Feng X (2006) Preparation and properties of trimesoyl chloride crosslinked poly(vinyl alcohol) membranes for pervaporation dehydration of isopropanol. J Membr Sci 286:245–254. doi:10.1016/j.memsci.2006.09.042
3. Sahmetlioglu E, Yuruk H, Toppare L, Cianga I, Yacci Y (2004) Synthesis and characterization of conducting copolymers of poly(vinyl alcohol) with thiophene side-groups and pyrrole. Polym Int 53:2138–2144. doi:10.1002/pi.1644
4. Yang JM, Su YW, Leu TL, Yang MC (2004) Evaluation of chitosan/PVA blended hydrogel membranes. J Membr Sci 236:39–51. doi:10.1016/j.memsci.2004.02.005
5. Liu Z, Dong Y, Men H, Jiang M, Tong J, Zhou J (2012) Post-crosslinking modification of thermoplastic starch/PVA blend films by using sodium hexametaphosphate. Carbohydr Polym 89:473–477. doi:10.1016/j.carbpol.2012.02.076
6. Zhai M, Yoshii F, Kume T, Hashim K (2002) Syntheses of PVA/starch grafted hydrogels by irradiation. Carbohydr Polym 50:295–303. doi:10.1016/S0144-8617(02)00031-0
7. Yuan HK, Ren J, Ma XH, Xu ZL (2011) Dehydration of ethyl acetate aqueous solution by pervaporation using PVA/PAN hollow fiber composite membrane. Desalination 280:252–258. doi:10.1016/j.desal.2011.07.002
8. Zhao B, Lu CH, Liang M (2007) Solvent-free esterification of poly(vinyl alcohol) and maleic anhydride through mechanochemical reaction. Chin Chem Lett 18:1353–1356. doi:10.1016/j.cclet.2007.09.019
9. Shermergom IM, Kamardin YB (1965) Study of interfacial esterification of polyvinyl alcohol (PVA). Polym Sci U.S.S.R. 7:2364–2369. doi:10.1016/0032-3950(65)90177-2
10. Dave R, Madamwar D (2006) Esterification in organic solvents by lipase immobilized in polymer of PVA–alginate–boric acid. Process Biochem 41:951–955. doi:10.1016/j.procbio.2005.10.019
11. Elena VB, Anis A, Sri B, Alvarez ZE, Sammy LI, Chana V, Basiuk A (2009) Poly(vinyl alcohol)/CNT composites: an effect of cross-linking with glutaraldehyde. Superlatt Microstr 46:379–383. doi:10.1016/j.spmi.2008.10.007
12. Priscila MA, Rosemary AC, Izabel CFM, Carla GL, Ana-Mônica QB, Paulo JAS (2011) Development of films based on blends of gelatin and poly(vinyl alcohol), cross linked with glutaraldehyde. Food Hydrocoll 25:1751–1757. doi:10.1016/j.foodhyd.2011.03.018
13. Takei T, Ikeda K, Ijima H, Kawakami K (2011) Fabrication of poly(vinyl alcohol) hydrogel beads cross-linked using sodium sulfate for microorganism immobilization. Process Biochem 46:566–571. doi:10.1016/j.procbio.2010.10.011
14. Atta MA, Nermine EM, Arndt KF (2006) Swelling characteristics of pH and thermo-sensitive cross-linked polyvinyl alcohol grafts. J Polym Res 13:53–63. doi:10.1007/s10965-005-9004-z
15. Shafee EE, Naguib HF (2003) Water sorption in cross-linked poly(vinyl alcohol) networks. Polymer 44:1647–1653. doi:10.1016/S0032-3861(02)00865-0
16. Peng F, Lu L, Sun H, Wang Y, Liu J, Jiang Z (2005) Hybrid organic–inorganic membrane: solving the tradeoff between permeability and selectivity. Chem Mater 17:6790–6796. doi:10.1021/cm051890q
17. Shengju W, Fengting L, Hongtao W, Lin F, Bingru Z, Guangtao L (2010) Effects of poly (vinyl alcohol) (PVA) content on preparation of novel thiol-functionalized mesoporous PVA/SiO₂ composite nanofiber membranes and their application for adsorption of heavy metal ions from aqueous solution. Polymer 51:6203–6211. doi:10.1016/j.polymer.2010.10.015
18. Yoon SD, Chough SH, Park HR (2007) Preparation of resistant starch/poly(vinyl alcohol) blend films with added plasticizer and crosslinking agents. J Appl Polym Sci 106:2485–2493. doi:10.1002/app.26755
19. Uslu H, Daştan A, Altaş A, Yayli O, Atakol M, Aksu L (2007) Preparation and characterization of PVA/Boron polymer produced by an electrospinning technique. E-Polymer 133:1–6. doi:10.1007/s10965-011-9607-5

20. Zhang Y, Peter CZ, David E (2010) Crosslinking reaction of poly(vinyl alcohol) with glyoxal. J Polym Res 17:725–730. doi:10.1007/s10965-009-9362-z
21. Miyazaki T, Yuuki T, Sachiko A, Takahiko I, Akie H, Keiko E (2010) Role of boric acid for a poly (vinyl alcohol) film as a cross-linking agent: melting behaviors of the films with boric acid. Polymer 51:5539–5549. doi:10.1016/j.polymer.2010.09.048
22. Zhang HZ, Liu BL, Luo R, Wu Y, Lei D (2006) The negative biodegradation of poly(vinyl alcohol) modified by aldehydes. Polym Degrad Stab 91:1740–1746. doi:10.1016/j.polymdegradstab.2005.11.019
23. Peng Z, Kong LX (2007) A thermal degradation mechanism of polyvinyl alcohol/silica nanocomposites. Polym Degrad Stab 92:1061–1071. doi:10.1016/j.polymdegradstab.2007.02.012
24. Gupta B, Anjum S, Ikram S (2013) Prepration of thiolated polyvinyl alcohol hydrogels. J Appl Polym Sci 129:815–821. doi:10.1002/APP.38856
25. Gupta B, Anjum S, Ikram S (2013) Physicochemical studies of crosslinked thiolated polyvinyl alcohol hydrogels. Polym Bull. doi:10.1007/s00289-013-0965-5
26. Dominguez L, Yue Z, Economy J, Mangun CL (2002) Design of polyvinyl alcohol mercaptyl fibers for arsenite chelation. React Funct Polym 53:205–215. doi:10.1016/S1381-5148(02)00174-8
27. Gupta B, Agarwal R, Alam MS (2013) Preparation and characterization of polyvinyl alcohol-polyethylene oxide-carboxymethyl cellulose blend membranes. J Appl Polym Sci 127:1301–1308. doi:10.1002/app.37665
28. Hasimi A, Stavropoulou A, Papadokostaki KG, Sanopoulou M (2008) Transport of water in polyvinyl alcohol films: effect of thermal treatment and chemical crosslinking. Eur Polym J 44:4098–4107. doi:10.1016/j.eurpolymj.2008.09.011
29. Vázquez TH, Cauich RJV, Cruz RCA (1993) Poly(vinyl alcohol)/poly(acrylic acid) blends: miscibility studies by DSC and characterization of their thermally induced hydrogels. J Appl Polym Sci 50:777–792. doi:10.1002/app.1993.070500505
30. Tudorachia N, Cascaval N, Rusu M, Pruteanu M (2000) Testing of polyvinyl alcohol and starch mixtures as biodegradable polymeric materials. Polym Test 19:785–799. doi:10.1016/S0142-9418(99)00049-5
31. Sreedhar B, Sairam M, Chattopadhyay DK, Syamala RPA, Rao MDV (2005) Thermal, mechanical, and surface characterization of starch–poly(vinyl alcohol) blends and borax-crosslinked films. J Appl Polym Sci 96:1313–1322. doi:10.1002/app.21439
32. Berger J, Reist M, Mayer JM, Felt O, Peppas NA, Gurny R (2004) Structure and interactions in covalently and ionically crosslinked chitosan hydrogels for biomedical applications. Eur J Pharm Biopharm 57:19–34. doi:10.1016/S0939-6411(03)00161-9
33. Hidalgo M, Reinecke H, Mijangos C (199) PVC containing hydroxyl groups: II Characterization and properties of crosslinked polymers. Polymer 40:3535–3543. doi:10.1016/S0032-3861(98)00568-0
34. Woo JY, Shin EJ, Lee YH (2010) Effect of boric acid treatment on the crystallinity and drawability of poly(vinyl alcohol)–iodine complex films. Polym Bull 65:169–180. doi:10.1007/s00289-010-0279-9
35. Marini A, Berbenni V, Capsoni D, Riccardi R, Zerlia T (1994) Factors affecting the spectral response in a TG/FT-IR experiment. Appl Spectrosc 48:1468–1471. doi:0003-7028/94/4812-146852,0
36. Peng Z, Kong LX, Li SD (2005) Thermal properties and morphology of a poly(vinyl alcohol)/silica nanocomposite prepared with a self-assembled monolayer technique. J Appl Polym Sci 96:1436–1442. doi:10.1002/app.21583
37. Zhu HM, Yan JH, Jiang XG, Lai YE, Cen KF (2008) Study on pyrolysis of typical medical waste materials by using TG-FTIR analysis. J Hazard Mater 153:670–676. doi:10.1016/j.jhazmat.2007.09.011
38. Han L, Wang Q, Ma Q, Yu C, Luo Z, Cen K (2010) Influence of CaO additives on wheat-straw pyrolysis as determined by TG-FTIR analysis. J Anal Appl Pyrolys 88:199–206. doi:10.1016/j.jaap.2010.04.007
39. Tao L, Zhao G, Qian J, Qin Y (2010) TG–FTIR characterization of pyrolysis of waste mixtures of paint and tar slag. J Hazard Mater 175:754–761. doi:10.1016/j.jhazmat.2009.10.073
40. Jiang X, Li C, Chi Y, Yan J (2010) TG-FTIR study on urea-formaldehyde resin residue during pyrolysis and combustion. J Hazard Mater 173:205–2010. doi:10.1016/j.jhazmat.2009.08.070
41. Hanst PL, Hanst S (1993) Infrared spectra for quantitative analysis of gases. Infrared Analysis, Anaheim, CA
42. János M, Petra B, Masayuki O, Shoji K, György P (2004) Comparative online coupled TG-FTIR and TG/DTA-MS analyses of the evolved gases from thiourea complexes of

SnCl₂Tetrachloropenta(thiourea) ditin(II), a compound rich in thiourea. J Anal Appl Pyrolysis 72:209–214. doi:10.1016/j.jaap.2004.06.003

43. Gupta B, Anjum S, Ikram S (2013) Preparation of crosslinked thiolated poly(vinyl alcohol) hydrogels for arsenic removal from water. Polym Bull (Communicated)